

# An Adaptive IHS Pan-Sharpener Method

Sheida Rahmani, Melissa Strait, Daria Merkurjev, Michael Moeller, and Todd Wittman

**Abstract**—The goal of pan-sharpening is to fuse a low spatial resolution multispectral image with a higher resolution panchromatic image to obtain an image with high spectral and spatial resolution. The Intensity-Hue-Saturation (IHS) method is a popular pan-sharpening method used for its efficiency and high spatial resolution. However, the final image produced experiences spectral distortion. In this letter, we introduce two new modifications to improve the spectral quality of the image. First, we propose image-adaptive coefficients for IHS to obtain more accurate spectral resolution. Second, an edge-adaptive IHS method was proposed to enforce spectral fidelity away from the edges. Experimental results show that these two modifications improve spectral resolution compared to the original IHS and we propose an adaptive IHS that incorporates these two techniques. The adaptive IHS method produces images with higher spectral resolution while maintaining the high-quality spatial resolution of the original IHS.

**Index Terms**—Image fusion, intensity-hue-saturation (IHS) transformation, multispectral image, pan-sharpening, performance evaluations.

## I. INTRODUCTION

MANY satellites provide two types of images: high-resolution panchromatic and low-resolution multispectral. The multispectral image lacks high spatial quality and the panchromatic image has low spectral quality. Due to these restrictions, many pan-sharpening methods have been created to fuse the two images together to obtain an image with high spectral and high spatial resolutions. A few popular pan-sharpening methods are: IHS [1], PCA-based image fusion [2], wavelet-based image fusion [3], Brovey [4], and P+XS [5]. Each method experiences a tradeoff between spectral and spatial quality. Researchers have created variants of these methods to improve their spectral and spatial quality. In this letter, we propose new adaptations to the IHS method.

IHS-based methods are often used due to their simple computation, high spatial resolution and efficiency. The fused image results in high spatial resolution and low spectral resolution. Many modifications have been proposed to enhance its spectral quality.

The IHS fusion technique converts a color image from RGB space to the IHS color space. Here, the  $I$  (intensity) band is

replaced by the panchromatic image. The intensity band  $I$  is calculated using

$$I = \sum_{i=1}^N \alpha_i M_i$$

where  $M_i$  are the multispectral bands, and the standard value for  $\alpha$  in an RGB image is  $\alpha_i = 1/3$ . However, most multispectral images consist of four bands, RGB, and an infrared band. To address this issue, researchers have extended this method for other multispectral images by using  $\alpha_i = 1/N$  where  $N$  is the number of bands [6], [7]. For the IKONOS satellite, the coefficients  $\alpha$  were experimentally determined [8].

Before fusing the two images, first we upsample the multispectral image by a factor of four and we normalize each band of the image to the range [0, 1]. After completing the initial steps, we do a histogram matching of the panchromatic image  $P$  to ensure that the mean and standard deviation of the panchromatic image and multispectral image are within the same range using

$$P = \frac{\sigma_I}{\sigma_P} (P - \mu_P) + \mu_I$$

where  $\sigma$  and  $\mu$  are the standard deviation and mean, respectively. Finally, the fused multichannel image  $F$  is formed by

$$F_i = M_i + (P - I).$$

The final fused IHS image usually has high spatial but low spectral resolution. We propose an image-adaptive IHS method that produces high spectral resolution by finding image-adaptive  $\alpha$  coefficient. We also propose a method that extracts the edges of the panchromatic image and combines it with the multispectral image to increase the spectral quality. Finally, we propose an adaptive IHS that incorporates these techniques together to improve the quality of the fused image.

## II. MODIFICATIONS TO IHS

### A. Image Adaptive Coefficients

In order to minimize spectral distortion in the IHS pan-sharpened image, we propose a new modification of the IHS that varies the manner the intensity band is calculated depending on the initial multispectral and panchromatic images. To minimize spectral distortion the intensity band should approximate the panchromatic image as closely as possible. Therefore, in this adaptive IHS method we want to determine the coefficients  $\alpha$  that best approximate

$$P \approx \sum_{i=1}^N \alpha_i M_i.$$

Manuscript received March 4, 2010. Date of publication May 10, 2010; date of current version October 13, 2010. This work was supported by the U.S. Department of Defense.

The authors are with the Department of Mathematics at University of California at Los Angeles, CA 90095-1555 USA (e-mail: sheida\_r18@yahoo.com; mstrait@hmc.edu; katiadaria@mail.ru; M.Moeller@gmx.net; wittman@math.ucla.edu).

Digital Object Identifier 10.1109/LGRS.2010.2046715

In order to calculate these coefficients we create the following function  $G$  to minimize with respect to the  $\alpha$ :

$$\min_{\alpha} G(\alpha) = \sum_x \left( \sum_i (\alpha_i M_i(x) - P(x))^2 + \gamma \sum_i (\max(0, -\alpha_i))^2 \right).$$

The first term ensures that the coefficients yield a linear combination that approximates the panchromatic image. Physically we do not want negative  $\alpha$ , therefore we add the non-negativity constraint on the  $\alpha$  using the Lagrange multiplier  $\gamma$ . In order to solve this minimization problem we use a gradient descent method. Calculating the derivative with respect to  $\alpha$  gives

$$\frac{d}{d\alpha_n} G(\bar{\alpha}) = 2 \sum_x \left( \sum_{i=1}^N \alpha_i M_i(x) - P(x) \right) M_n(x) - 2\gamma \max(0, -\alpha_n).$$

We discretize the PDE to obtain a semi-implicit scheme

$$\frac{\alpha_n^{\tau+1} - \alpha_n^{\tau}}{\tau} = -2 \sum_x \left( \sum_{i=1}^N \alpha_i^{\tau+1} M_i(x) - P(x) \right) M_n(x) + 2\gamma \max(0, -\alpha_n).$$

Solving for  $\alpha_n^{t+1}$  gives

$$\begin{aligned} \alpha_n^{t+1} + 2\tau \sum_{i=1}^N \left[ \left( \sum_x (M_i(x) M_n(x)) \right) \alpha_i^{t+1} \right] \\ = \alpha_n^t + 2\tau \sum_x (P(x) M_n(x)) + 2\tau\gamma \max(0, -\alpha_n^t). \end{aligned}$$

This equation can be solved quickly by linear algebra methods. Calculating the coefficients in this manner increases the spectral quality of the images because it generates coefficients according to the original data, and maintains the good spatial quality of the IHS method.

### B. Edge-Adaptive IHS

In this method, we want to transfer the edges from the panchromatic image to the fused image. This approach extracts the edges from the panchromatic image; where there are edges, the IHS method was imposed; otherwise, the multispectral image was used. The fused multichannel image  $F$  is formed by the new formula:

$$F_i = M_i + h(x)(P - I)$$

where  $h(x)$  is an edge detecting function. We want  $h(x)$  to equal to 1 on edges and equal to zero off edges. The extracted edge can be obtained using standard edge detection methods such as they Canny detector [9]. We found experimentally that the best results were produced by the edge detector suggested by Perona and Malik [10]. The edges of the panchromatic image are extracted using an exponential edge detector

$$h(x) = \exp \left( -\frac{\lambda}{|\nabla P|^4 + \varepsilon} \right)$$

where  $\nabla P$  is the gradient of the panchromatic image,  $\lambda$  is a parameter indicating how large the gradient should be in order to be an edge and controls the smoothness of the image, and  $\varepsilon$  is a small value that enforces a nonzero denominator [11].

The values that proved successful are  $\lambda = 10^{-9}$  and  $\varepsilon = 10^{-10}$ . Using these values and combining the edge detection with the original IHS increases the spectral resolution significantly.

### C. Adaptive IHS

Due to the high performance of the edge-adaptive method and image-adaptive coefficient method, we also present a method that combines these two techniques. The integration of these two techniques with IHS we call adaptive IHS. This method preserves the high spatial quality and increases the spectral quality. In this method, the  $\alpha_i$ 's are computed to create the I band, and the edge detection formula  $h(x)$  is inserted as well to compute the final fused image. We compare the performance of these three methods in the following section.

## III. RESULTS

Four-band multispectral QuickBird and LANDSAT data was used for our experiments. The algorithms were implemented in Matlab. The software and documentation is available online at: [www.math.ucla.edu/~wittman/pansharpening](http://www.math.ucla.edu/~wittman/pansharpening).

The original IHS, edge-adaptive, image-adaptive, stationary Wavelet, PCA, and adaptive IHS methods are being compared for their spectral and spatial quality. Spatial quality can be judged visually, but subtle color changes are more difficult to notice in this manner. Therefore, we consult performance metrics in order to evaluate the spectral quality. Since high-resolution ground truth was not available, we compared the fusion results against an upsampled version of the original data.

We use several different metrics to help us analyze our results. Spectral Angle Mapper (SAM) calculates the average change in angle of all spectral vectors [12]. Spectral Information Divergence (SID) views each pixel spectrum as a random variable and then measures the discrepancy of probabilistic behaviors between spectra [13]. A Universal Image Quality Index (Q-average) models any distortion as a combination of three different factors: loss of correlation, luminance distortion, and contrast distortion [14], [15]. The relative average spectral error (RASE) characterizes the average performance of the method of image fusion in the spectral bands [16]. We also used the root mean squared error (RMSE) and correlation coefficient (CC) to analyze and compare the spectral quality [17]. The CC calculates the spectral distortion by comparing the CC between the original multispectral bands and the bands of the final fused image. RMSE is the root mean square error between the fused image and the multispectral image. Relative dimensionless global error in synthesis (ERGAS) is a normalized version of RMSE designed to calculate the spectral distortion [18].

In Figs. 1–4, the IHS and adaptive IHS methods both clearly sharpen the original image and greatly improve the spatial quality. In Figs. 1 and 2, the spectral distortion of the standard IHS method is most visible in the blue color of the swimming



Fig. 1. Pan-sharpening a suburban QuickBird scene. Copyright DigitalGlobe, NextView license, 2003.

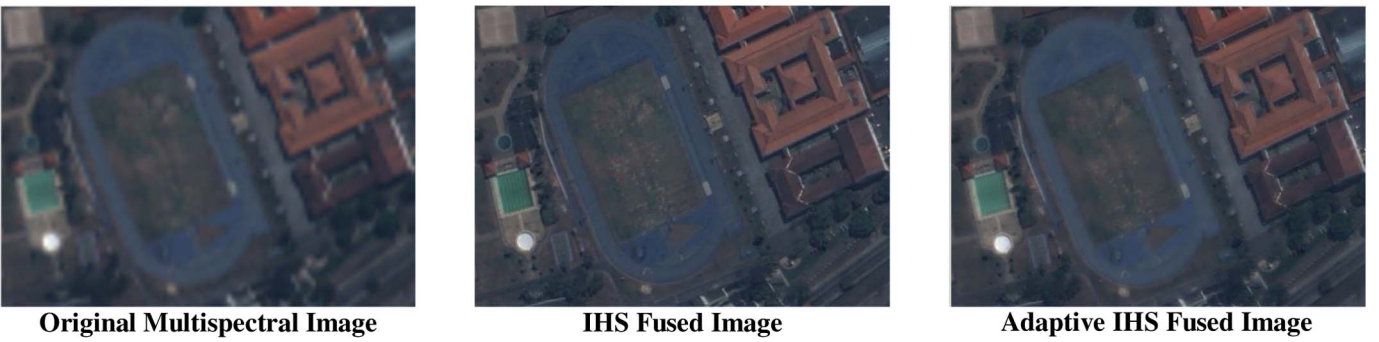


Fig. 2. Pan-sharpening an urban QuickBird scene. Copyright DigitalGlobe, NextView license, 2003.



Fig. 3. Pan-sharpening a rural LANDSAT-7 scene in Sioux Falls, SD. Source: USGS, [www.americaview.org](http://www.americaview.org).



Fig. 4. Pan-sharpening a forest QuickBird scene. Copyright DigitalGlobe, NextView license, 2003.

TABLE I  
SPECTRAL QUALITY METRICS FOR FIG. 1

|                    | CC     | ERGAS  | Qave   | RASE    | RMSE   | SAM    | SID    |
|--------------------|--------|--------|--------|---------|--------|--------|--------|
| Reference Values   | 0      | 0      | 1      | 0       | 0      | 0      | 0      |
| Original IHS       | 0.0509 | 3.1528 | 0.9439 | 12.4210 | 0.0544 | 1.1878 | 0.0139 |
| Edge Adaptive IHS  | 0.0373 | 2.8496 | 0.9549 | 11.2628 | 0.0493 | 0.9505 | 0.0132 |
| Image Adaptive IHS | 0.0085 | 2.3444 | 0.9705 | 9.2362  | 0.0405 | 0.7043 | 0.0026 |
| Adaptive IHS       | 0.0104 | 2.2425 | 0.9731 | 8.8277  | 0.0387 | 0.6050 | 0.0021 |
| PCA                | 0.2673 | 4.5562 | 0.8636 | 17.6634 | 0.0774 | 2.8223 | 0.0212 |
| Stationary Wavelet | 0.0184 | 1.7341 | 0.9840 | 6.8419  | 0.0300 | 0.7383 | 0.0013 |

TABLE II  
SPECTRAL QUALITY METRICS FOR FIG. 2

|                    | CC     | ERGAS  | Qave   | RASE    | RMSE   | SAM    | SID    |
|--------------------|--------|--------|--------|---------|--------|--------|--------|
| Reference Values   | 0      | 0      | 1      | 0       | 0      | 0      | 0      |
| Original IHS       | 0.0433 | 2.7883 | 0.9006 | 10.7874 | 0.0320 | 0.8262 | 0.0017 |
| Edge Adaptive IHS  | 0.0218 | 2.4429 | 0.9256 | 9.4623  | 0.0280 | 0.5585 | 0.0014 |
| Image Adaptive IHS | 0.0144 | 2.1205 | 0.9466 | 8.2036  | 0.0243 | 0.5621 | 0.0006 |
| Adaptive IHS       | 0.0056 | 1.9305 | 0.959  | 7.4694  | 0.0221 | 0.4061 | 0.0004 |
| PCA                | 0.3007 | 2.9509 | 0.8985 | 11.9893 | 0.0355 | 1.6822 | 0.0041 |
| Stationary Wavelet | 0.0237 | 1.4905 | 0.9740 | 5.8244  | 0.0173 | 0.5902 | 0.0004 |

TABLE III  
SPECTRAL QUALITY METRICS FOR FIG. 3

|                    | CC     | ERGAS  | Qave   | RASE   | RMSE   | SAM    | SID    |
|--------------------|--------|--------|--------|--------|--------|--------|--------|
| Reference Values   | 0      | 0      | 1      | 0      | 0      | 0      | 0      |
| Original IHS       | 0.0025 | 1.1433 | 0.9698 | 4.5688 | 0.0263 | 0.0673 | 0.0006 |
| Edge Adaptive IHS  | 0.0018 | 1.0831 | 0.9728 | 4.3274 | 0.0249 | 0.0583 | 0.0005 |
| Image Adaptive IHS | 0.0008 | 1.0815 | 0.9730 | 4.3220 | 0.0249 | 0.0615 | 0.0006 |
| Adaptive IHS       | 0.0008 | 1.0302 | 0.9755 | 4.1169 | 0.0237 | 0.0537 | 0.0005 |
| PCA                | 0.1044 | 2.4431 | 0.7902 | 9.7709 | 0.0563 | 0.4432 | 0.0037 |
| Stationary Wavelet | 0.0044 | 0.8965 | 0.9817 | 3.5823 | 0.0206 | 0.4510 | 0.0014 |

TABLE IV  
SPECTRAL QUALITY METRICS FOR FIG. 4

|                    | CC     | ERGAS  | Qave   | RASE    | RMSE   | SAM    | SID    |
|--------------------|--------|--------|--------|---------|--------|--------|--------|
| Reference Values   | 0      | 0      | 1      | 0       | 0      | 0      | 0      |
| Original IHS       | 0.0209 | 5.6819 | 0.6501 | 21.5700 | 0.0909 | 2.2080 | 0.0148 |
| Edge Adaptive IHS  | 0.0183 | 5.3771 | 0.6757 | 20.5317 | 0.0866 | 2.0158 | 0.0142 |
| Image Adaptive IHS | 0.0282 | 4.9675 | 0.7264 | 18.8583 | 0.0795 | 1.9770 | 0.0171 |
| Adaptive IHS       | 0.0345 | 4.7133 | 0.7475 | 17.9718 | 0.0758 | 1.8134 | 0.0166 |
| PCA                | 0.2729 | 5.4004 | 0.6006 | 19.6502 | 0.0828 | 3.2349 | 0.0192 |
| Stationary Wavelet | 0.0162 | 2.0208 | 0.9571 | 7.6711  | 0.0323 | 1.0061 | 0.0124 |

pool and running track. The adaptive IHS method produces an image whose colors better match the original image. Spectral distortion is also visible in the forest shown in Fig. 4. The shadows in the trees are more precise and darker in the adaptive IHS method than in the original.

Next we look at the metrics to evaluate the spectral quality. We want the metrics to correspond to our prediction of the methods. The values in Tables I–IV correspond to the images in Figs. 1–4, respectively. In all tables, the values of the metrics

are closer to the optimal value when using the adaptive IHS. The image- adaptive and edge-adaptive both perform better than the original IHS. Combining the techniques achieves even better results. Note that the values in Tables I and II show more improvement than Tables III and IV. This is because the images corresponding to the last two tables are rural scenes and there are fewer strong edges to sharpen than in an urban or suburban scene. We also show the results for the Stationary Wavelet and PCA methods. The performance of IHS is consistently better

than PCA. Comparing to Stationary Wavelet, the metrics are close to IHS. The spectral quality of the wavelet method is usually better, but the tradeoff is that the Stationary Wavelet method is much slower to compute and the fused image often has lower visual quality than images produced by the IHS methods.

#### IV. CONCLUSION

The IHS pan-sharpening method gives good spatial quality and is a commonly used algorithm for its speed and simplicity. To improve its spectral quality we proposed two new techniques: edge-adaptive and image-adaptive. The merging of these techniques improves the spectral quality of the IHS-fused image while maintaining its spatial resolution. Therefore, we proposed the adaptive IHS that incorporates both of these techniques, which in turn presents the best spectral quality among these methods. The performance evaluation metrics confirmed the competence of the adaptive IHS method.

#### ACKNOWLEDGMENT

The authors would like to thank Prof. A. Bertozzi for her advice and assistance.

#### REFERENCES

- [1] T. Tu, S. Su, H. Shyn, and P. Huang, "A new look at IHS-like image fusion methods," *Inf. Fusion*, vol. 2, no. 3, pp. 177–186, Sep. 2001.
- [2] V. P. Shah and N. H. Younan, "An efficient pan-sharpening method via a combined adaptive PCA approach and contourlets," *IEEE Trans. Geosci. Remote Sens.*, vol. 46, no. 5, pp. 1323–1335, May 2008.
- [3] X. Otazu and M. Gonzalez-Ausciana, "Introduction of sensor spectral response into image fusion methods: Application to wavelet-based methods," *IEEE Trans. Geosci. Remote Sens.*, vol. 43, no. 10, pp. 2376–2385, Oct. 2005.
- [4] A. Eshtehari and H. Ebadi, *Image Fusion of Landsat ETM+ and Spot Satellite Images Using IHS, Brovey and PCA*. Tehran, Iran: Toosi Univ. Technol., 2008.
- [5] C. Ballester, V. Caselles, L. Igual, and J. Verdera, "A variational model for P + XS image fusion," *Int. J. Comput. Vis.*, vol. 69, no. 1, pp. 43–58, Aug. 2006.
- [6] Y. Zhang, *Understanding Image Fusion*. Richmond Hill, ON, Canada: PCI Geomatics, 2008.
- [7] M. Choi, "A new intensity-hue-saturation fusion approach to image fusion with a tradeoff parameter," *IEEE Trans. Geosci. Remote Sens.*, vol. 44, no. 6, pp. 1672–1682, Jun. 2006.
- [8] M. Choi, H. Kim, N. I. Cho, and H. O. Kim, "An improved intensity-hue-saturation method for IKONOS image fusion," Korea Adv. Inst. Sci. Technol., Daejeon, Korea, Tech. Rep. 06-9, 2008.
- [9] J. Canny, "A computational approach to edge detection," *IEEE Trans. Pattern Anal. Mach. Intell.*, vol. PAMI-8, no. 6, pp. 679–698, Nov. 1986.
- [10] P. Perona and J. Malik, "Scale-space and edge detection using anisotropic diffusion," *IEEE Trans. Pattern Anal. Mach. Intell.*, vol. 12, no. 7, pp. 629–639, Jul. 1990.
- [11] H. Aanaes and J. Sveinsson, "Model-based satellite image fusion," *IEEE Trans. Geosci. Remote Sens.*, vol. 46, no. 5, pp. 1336–1346, May 2008.
- [12] A. Goetz, W. Boardman, and R. Yunas, "Discrimination among semi-arid landscape endmembers using the Spectral Angle Mapper (SAM) algorithm," in *Proc. Summaries 3rd Annu. JPL Airborne Geosci. Workshop*, 1992, pp. 147–149.
- [13] C.-I. Chang, "Spectral information divergence for hyperspectral image analysis," in *Proc. IEEE Int. Geosci. Remote Sens. Symp.*, 1999, vol. 1, pp. 509–511.
- [14] A. Bovik and Z. Wang, "A universal image quality index," *IEEE Signal Process. Lett.*, vol. 9, no. 3, pp. 81–84, Mar. 2002.
- [15] L. Alparone, B. Aiuzzi, S. Baronti, A. Garzelli, and P. Nencini, "A global quality measurement of pan-sharpened multispectral imagery," *IEEE Geosci. Remote Sens. Lett.*, vol. 1, no. 4, pp. 313–317, Oct. 2004.
- [16] M. Choi and R. Kim, "Fusion of multispectral and panchromatic satellite images using the curvelet transforms," *IEEE Geosci. Remote Sens. Lett.*, vol. 2, no. 2, pp. 136–140, Apr. 2005.
- [17] Q. Du, O. Gungor, and J. Shan, *Performance Evaluation for Pan-Sharpening Techniques*. Mississippi State, MS: Dept. Elect. Comput. Eng., Mississippi State Univ., Jun. 24, 2008.
- [18] L. Wald, "Quality of high resolution synthesized images: Is there a simple criterion," in *Proc. Int. Conf. Fusion Earth Data*, 2000, pp. 99–105.